1521-009X/47/10/1136–1145$35.00
Drug Metabolism and Disposition

https://doi.org/10.1124/dmd.119.087809
Drug Metab Dispos 47:1136–1145, October 2019

Special Section on Pharmacokinetic and Drug Metabolism Properties of Novel Therapeutic Modalities

Effect of Size on Solid Tumor Disposition of Protein Therapeutics

Zhe Li, Yingyi Li, Hsuan-Ping Chang, Hsueh-Yuan Chang, Leiming Guo, and Dhaval K. Shah

Department of Pharmaceutical Sciences, School of Pharmacy and Pharmaceutical Sciences, The State University of New York at Buffalo, Buffalo, New York

Received May 2, 2019; accepted July 22, 2019

ABSTRACT

In this study, we evaluated the effect of size on tumor disposition of protein therapeutics, including the plasma and tumor pharmacokinetics (PK) of trastuzumab (~150 kDa), FcRn-nonbinding trastuzumab (~150 kDa), F(ab)$_2$ fragment of trastuzumab (~100 kDa), Fab fragment of trastuzumab (~50 kDa), and trastuzumab scFv (~27 kDa) in both antigen (i.e., HER2)-overexpressing (N87) and antigen-nonexpressing (MDA-MB-468) tumor-bearing mice. The observed data were used to develop the maximum tumor uptake versus molecular weight and tumor-to-plasma area under the curve (AUC) ratio versus molecular weight relationships. Comparison of the PK of different sizes of FcRn nonbinding molecules in target-expressing tumor showed that ~100 kDa is an optimal size to achieve maximum tumor uptake and ~50 kDa is an optimal size to achieve maximum tumor-to-plasma exposure ratio of protein therapeutics. The PK data were also used to validate a systems PK model for tumor disposition of different-sized protein therapeutics. The PK model was able to predict *a priori* the PK of all five molecules in both tumor types reasonably well (within 2- to 3-fold). In addition, the model captured the bell-shaped relationships observed between maximum tumor uptake and molecular weight and between tumor-to-plasma AUC ratio and molecular weight. Our results provide an unprecedented insight into the effect of size and target engagement on the tumor PK of protein therapeutics. Our results also provide further validation of the tumor disposition model, which can be used to support discovery, development, and preclinical-to-clinical translation of different sizes of protein therapeutics.

SIGNIFICANCE STATEMENT

This article highlights the importance of molecular size and target engagement on the tumor disposition of protein therapeutics. Our results suggest that ~100 kDa is an optimal size to achieve maximum tumor uptake and ~50 kDa is an optimal size to achieve maximum tumor-to-plasma exposure ratio for non-FcRn-binding targeted protein therapeutics. We also demonstrate that a systems pharmacokinetics model developed to characterize tumor disposition of protein therapeutics can predict a priori the disposition of different-sized protein therapeutics in target-expressing and target-nonexpressing solid tumors.

Introduction

Decades of thorough research has greatly improved our understanding of the pharmacokinetics (PK) of antibody-based therapeutics (Wang et al., 2008); however, solid tumor disposition of antibodies and other protein therapeutics remains less well understood. Since the exposure of protein therapeutics in the tumor is not always proportional to the systemic exposure, and the information about the exposure at the site of action is crucial for developing an effective therapeutic or diagnostic agent, it is important to understand and predict the effect of different factors that determine the solid-tumor PK of protein therapeutics (Scott et al., 2012).

Tumor penetration of antibodies/protein therapeutics is generally determined by both tumor-specific and drug-specific factors. (Scott et al., 2012; Glassman and Balthasar, 2014) Typical tumor-specific barriers include high interstitial pressure, abnormal blood vasculature, extracellular matrix components, and heterogeneous distribution of cancer cell surface antigen. Drug-specific factors include serum half-life, target-mediated drug disposition in the tumor, and protein size. Of these factors, size plays an important role because it affects overall tumor exposure by affecting both systemic PK (Li et al., 2016, 2017) and tumor penetration of protein therapeutics (Beckman et al., 2007; Thurber et al., 2007, 2008b). To date, however, there is no consensus on whether there is an optimal molecular size for targeting protein therapeutics to solid tumor. One pioneer work done by Schmidt and Wittrup (2009) used data from the literature from PK studies of different sizes of anti-HER2 molecules in mice and anticarcinoembryonic antigen molecules in humans to suggest that there is a "U"-shape relationship between maximum tumor uptake and protein molecular size. In addition, their study used data from the literature and mathematical modeling to suggest that tumor disposition is least efficient for protein therapeutics with an intermediate size of ~50 kDa; however, these results stemmed

This research was funded by grants from the Center for Protein Therapeutics (CPT) at the University at Buffalo and the National Institutes of Health (NIH), Grant number GM114179 and AI138195, awarded to Dr. D.K.S.
https://doi.org/10.1124/dmd.119.087809.
This article has supplemental material available at dmd.aspetjournals.org.

ABBREVIATIONS: AUC, area under the curve; CHO, Chinese haamsrer ovary; CL, clearance; ELISA, enzyme-linked immunosorbent assay; FcRn, neonatal Fc receptor; HER2, human epidermal growth factor receptor 2; PK, pharmacokinetics; SPR, surface plasmon resonance.

from a diverse set of data, generated in different studies, using different targeted molecules, under different experimental designs, and with the help of different bioanalytical methods. In addition, these results have not been validated by other groups. Consequently, in this study, we performed a dedicated preclinical study to understand the role of molecular size on tumor disposition of protein therapeutics.

In this study, we evaluated the effect of molecular size by investigating systemic and tumor PK of trastuzumab (~150 kDa), FcRn-nonbinding trastuzumab (~150 kDa), F(ab)$_2$ fragment of trastuzumab (~100 kDa), Fab fragment of trastuzumab (~50 kDa), and trastuzumab scFv (~27 kDa) in antigen-expressing (N87) and antigen-negative (MDA-MB-468) tumor-bearing mice. The observed data were used to develop "maximum tumor uptake versus protein size" and "tumor-to-plasma exposure ratio versus protein size" relationships. To understand more completely the underlying process that governs tumor disposition of different-sized antibody/fragments, the observed data were also characterized using a validated systems PK model that can predict a priori the tumor concentration of different-sized antibody/fragments. The PK model was also subjected to local sensitivity analysis to identify the most sensitive parameters that determine tumor disposition of different sizes of protein therapeutics.

Materials and Methods

Production and Characterization of Different Protein Therapeutics

Trastuzumab (Herceptin; Genentech, South San Francisco, CA) was purchased from a local hospital as a commercially packaged lyophilized powder, which contains excipients such as L-lysine, a,a-trehalose dihydrate, and Tween 20. There excipients improve the stability of the protein molecule after reconstitution. The other four proteins, which included FcRn nonbinding trastuzumab (150 kDa), F(ab)$_2$ (100 kDa), Fab (50 kDa), and scFv (27 kDa) fragment of trastuzumab, were generated inhouse.

Preparation of FcRn-Nonbinding Trastuzumab. The DNA sequence of trastuzumab and FcRn-nonbinding three-point mutations within CH domain (I136A, H193A, H318A) were obtained from the literature. The DNA sequence of FcRn-nonbinding trastuzumab was synthesized by Genscript and cloned into expression vector pcDNA5_FRT (Life Technologies, Carlsbad, CA). After transfection, positive Chinese hamster ovary cells were selected by adding 1 mg/ml hygromycin B in the medium. After ~10 days of growth, the cells were subcloned in 96-well plates for two rounds to separate the monoclones. Supernatant of each well was collected to determine [by enzyme-linked immunosorbent assay (ELISA)] the best clone. Then, the two best clones were acclimated and scaled up in 2-liter shaking flask using SFM-CD Chinese hamster (CHO) media (Gibco, Waltham, MA). The supernatant was collected and purified using HiTrap Protein G HP antibody purification column (GE Healthcare Life Sciences, Chicago, IL). The final product was buffer exchanged in PBS before the experiment.

Preparation of Fab Fragment of Trastuzumab. The Fab fragment of trastuzumab was generated in the laboratory using a commercially available papain-based digestion kit, followed by purification using a hydroxyapatite column. Briefly, 4 mg of trastuzumab was first purified using the Zeba Spin Desalting column (Thermo Fisher Scientific, Waltham, MA) by centrifugation at 1000*g* for 2 minutes (three times totally). Then, purified trastuzumab was incubated with 0.125 ml of papain-immobilized resin in 0.5 ml of digestion buffer (Thermo Fisher Scientific) at 37°C for 12 hours in a microcentrifuge tube. After digestion, the product was separated from immobilized papain by centrifuge at 5000*g* for 1 minute. The eluent mostly contained digested fragments (Fab and Fc) and a small amount of undigested trastuzumab. The mixture was purified using the hydroxyapatite column (Bio-Rad, Hercules, CA). Two elution buffers were used. Buffer A contained 10 mM sodium phosphate and 5 ppm calcium chloride, pH 6.5. Buffer B contained 500 mM sodium phosphate and 5 ppm calcium chloride, pH 6.5. The separation condition was optimized by changing the gradient of two eluent buffers. The identity of each peak from the chromatogram was determined using gel electrophoresis (SDS-PAGE). The final product was buffer exchanged in PBS before the experiment.

Preparation of F(ab)$_2$ Fragment of Trastuzumab. As with Fab generation, the F(ab)$_2$ fragment of trastuzumab was generated in the laboratory using a commercially available pepsin-based digestion kit, followed by purification using a hydroxyapatite column. Briefly, 4 mg of trastuzumab was first purified using the Zeba Spin Desalting column (Thermo Scientific) by centrifugation at 1000*g* for 2 minutes (three times totally). Then, purified trastuzumab was incubated with 0.125 ml of pepsin-immobilized resin in 0.5 ml of digestion buffer (Thermo Scientific) at 37°C for 8 hours in a microcentrifuge tube. After digestion, the product was separated from immobilized pepsin by centrifuge at 5000*g* for 1 minute. Then, the mixture was purified using the hydroxyapatite column (Bio-Rad). Two elution buffers were used. Buffer A contained 10 mM sodium phosphate and 5 ppm calcium chloride, pH 6.5. Buffer B contained 500 mM sodium phosphate and 5 ppm calcium chloride, pH 6.5. The separation condition was optimized by changing the gradient of two eluent buffers. The identity of separation products was determined using SDS-PAGE. The final product was buffer exchanged in PBS before the experiment.

Preparation of scFv Fragment of Trastuzumab. The sequence of scFv plasmid was designed by linking the sequences of VH and VL region of trastuzumab with the sequence of a polyglycine linker $(GGGGS)_3$. Two restriction enzyme sites for NheI and BamHI were included at the beginning and at the end of the sequence, respectively. After the plasmid was synthesized by Genscript (Nanjing, China), double-enzyme restriction for the scFv plasmid and an expression plasmid pcDNA5_FRT was done using NheI and BamHI (New England Biolabs, Ipswich, MA) by incubating them at 37°C for 2–4 hours. After enzyme restriction, the cDNA products from both the scFv plasmid and the pcDNA5_FRT plasmid were collected and ligated using the T4 ligation system (QIAGEN, Hilden, Germany) by incubating them at 16°C for 1 to 2 hours. After ligation, the plasmid was transfected into the competent *Escherichia coli*, Top10 (Invitrogen, Waltham, WA). After amplification, plasmid was extracted from *E. coli* using the Plasmid Mini Kit (QIAGEN) and used for CHO cell transfection. Two plasmids were transfected into CHO cells: the scFv-FRT plasmid and the pOG44 plasmid (Invitrogen). The transfected CHO cells were then subcloned in 96-well plates for two rounds to separate monoclones. Supernatant of each well was collected to determine the best clone by ELISA. The two best clones were amplified in T-75 flasks using SFM-CD CHO media. After the cell culture became highly confluent (~10 days), the supernatant was collected, and the scFv was purified using the His Gravitrap column (GE Healthcare Life Sciences). The identity of scFv was verified using SDS-PAGE gel analysis and Western blotting analysis. The final product was buffer exchanged in PBS before the experiment.

HER2-Binding Affinity of Trastuzumab, FcRn-Nonbinding Trastuzumab, F(ab)$_2$, Fab, and scFv Using Surface Plasmon Resonance. The antigen-binding property of trastuzumab, FcRn-nonbinding trastuzumab, F(ab)$_2$, Fab, and scFv were determined using surface plasmon resonance (SPR). Carboxymethyl dextran hydrogel surface sensor chips were purchased from Reichert Technologies (Depew, NY). The chip was first activated with 1-ethyl-3-(3-dimethylaminopropyl)-carbodiimide and N-hydroxysuccinimide. Then, 50 μg/ml protein in sodium acetate (10 mM, pH 5.0–5.5) was injected over the left channel until the desired immobilization level was reached (~600–1000 μRIU). After protein immobilization, all remaining reaction sites on the chip surface were blocked by flowing through ethanolamine (1 M, pH 8.5) for 10 minutes at 25 μl/min. Then, the chip was stabilized overnight by being run through blank running buffer (PBS-Tween buffer) or until the signal was stabilized. For each protein, the binding assay was conducted as follows. Eight concentrations (0.5, 2.5, 5, 10, 50, 200, 500, and 1000 nM) were tested. The protein samples were allowed to bind to the chip surface by flowing over both channels for 4 minutes and then dissociated for 30 minutes. After each binding cycle, the chip was regenerated using glycine buffer (10 mM, pH 2.0). Each concentration was run in triplicate. The binding sensorgrams were sent to BIAevaluation software (GE Healthcare), and the binding parameters were estimated in the software.

Analytical Method Development for Different Protein Therapeutics

Development of ELISA Method to Quantify Trastuzumab, F(ab)$_2$, and Fab in Mouse Plasma. Plasma obtained from N87 tumor-bearing nude mice was used to build standard curves for trastuzumab (300× dilution), F(ab)$_2$ (300× dilution), and Fab (50× dilution). Goat antihuman IgG (F(ab)$_2$ specific, cross-adsorbed) F(ab)$_2$ (Bethyl) was diluted to 5 μg/ml in PBS. Nunc Maxisorp 384-well plate was then coated with the diluted antibody (60 μl per well) and incubated at 4°C overnight. Plates were washed three times with PBS-Tween (0.05% Tween 20 in 1× PBS), followed by three washes with distilled water. Plates were then blocked with 90 μl/well of ELISA blocking solution and then incubated at room temperature for 1 hour. Plates were washed to remove the ELISA block solution later. Serial dilutions of trastuzumab, F(ab)$_2$, or Fab were made and ranged from 1000 to 3.9 ng/ml in prediluted plasma samples to act as standards. Plates were then incubated in triplicates (35 μl) for 2 hours at room temperature. After the

incubation period was over, plates were washed as described already herein. Later, 35 μl of goat antihuman IgG ($F(ab)_2$-specific, AP-conjugated, cross-adsorbed) $F(ab)_2$ (Bethyl) was added to each well, and the plate was incubated at room temperature for 1 hour. Plate was washed as described earlier, and p-nitro phenyl phosphate solution (1 mg/ml in diethanolamine buffer) was added to each well (60 μl). The change in absorbance was observed with time (dA/dt) at 405 nm with Filter Max F-5 microplate analyzer (Molecular Devices, San Jose, CA).

Development of ELISA Method to Quantify scFv in Mouse Plasma. The mouse plasma was diluted for 10× to build a standard curve for scFv. Recombinant human HER2 (5 μg/ml) was coated on the plate as the capture protein. Anti-His antibody (AP-conjugated; Abcam, Cambridge, UK) was used as the secondary antibody. All other steps were the same as described in the previous section.

Development of ELISA Method to Quantify Trastuzumab, $F(ab)_2$, Fab, and scFv in Tumor. N87 tumors taken from xenograft-bearing nude mice were used to create the standard curves. The tumor was weighed and homogenized in 5× v/w PBS with 1× protease inhibitor, using zironium beads and shaker (BeadBug, Sigma-Aldrich, St. Louis, MO). Homogenized tumor mixture was stored at −80°C until analysis. To build standard curves for trastuzumab, $F(ab)_2$, Fab, and scFv, tumor homogenate was further diluted by 20× using RIPA buffer (ThermoFisher) containing 1× protease inhibitor. The diluted mixture was used to prepare serial dilution of each molecule, ranging from 1000 to 4 nM. The standard solutions were then incubated on ice for 1 hour. All other steps were the same as described in the previous sections.

In Vivo PK Study in Tumor-Bearing Animals

Development of Mouse Xenograft Models with Two Cell Lines. All animal procedures were approved by the Institutional Animal Care and Use Committee at the State University of New York at Buffalo. Male athymic nude mice (Jackson Laboratory, Farmington, CT) were injected s.c. with ~10 million N87 or ~10 million MDA-MB-468 cells in the right flank region. After the average size of tumor reached ~300 mm^3, in vivo studies were conducted. The age of all mice at the time of the PK experiment is around 10 weeks. The tumor size was calculated using eq. 1:

$$Tumor\ size\ (mm^3) = 0.5 \times length\ (mm) \times width\ (mm) \times width\ (mm) \quad (1)$$

In Vivo Study to Determine Plasma and Tumor PK of Proteins in N87 Tumor-Bearing Mice. The plasma and tumor PK of all five molecules were investigated in N87 tumor-bearing nude mice at a 10-mg/kg dose. Each molecule was injected via penile vein in each mouse. Four terminal sampling time points were chosen for each molecule, and three animals were sacrificed at each time point. For IgG, the time points were 6, 24, 72, and 168 hours. For $F(ab)_2$, the time points were 1, 6, 24, and 48 hours. For Fab, the time points were 10 minutes 1, 4, and 24 hours. For scFv, the time points were 5 minutes, 1, 4, and 24 hours. At each predetermined time point, a blood sample was collected through cardiac puncture, and plasma was immediately separated via centrifugation (2000*g*, 20 minutes). After blood collection, whole-body perfusion was performed on each mouse to get rid of residual blood in the tumor, and tumor samples were collected at the end of perfusion. Collected plasma and tumor samples were stored at -80°C until analysis.

In Vivo Study to Determine Plasma and Tumor PK of Proteins in MDA-MB-468 Tumor-Bearing Mice. The plasma and tumor PK of all five molecules in MDA-MB-468 tumor-bearing nude mice was investigated using the same procedure described in the previous section.

Mathematical Modeling

Model Structure and Equations. Figure 1 shows the schematic of the PK model used to characterize the disposition of five different-sized molecules in solid tumor. The model contains a two-compartment PK model to characterize the systemic PK of each molecule. The tumor disposition model is connected to the central compartment of the two-compartment PK model, which is adapted from a more sophisticated mechanistic model that can describe the tumor penetration of protein molecules through both vascular extravasation and diffusion processes (Thurber et al., 2008a). Equations for the model are provided below (eqs. 2–8). A glossary of the terms used in model equations is provided in Table 1.

$$\frac{dX1}{dt} = -(CLD + CL) \times C1 + CLD \times C2 - \frac{2 \times P \times R_{cap}}{R_k{}^2} \times \left(C1 - \frac{C3}{\varepsilon}\right) \times TV - \frac{6 \times D}{R_t{}^2} \times \left(C1 - \frac{C3}{\varepsilon}\right) \times TV, \text{IC} = \text{Dose} \quad (2)$$

$$\frac{dX2}{dt} = CLD \times (C1 - C2) \quad , \text{IC} = 0 \quad (3)$$

$$\frac{dC3}{dt} = \frac{2 \times P \times R_{cap}}{R_k{}^2} \times \left(C1 - \frac{C3}{\varepsilon}\right) + \frac{6 \times D}{R_t{}^2} \times \left(C1 - \frac{C3}{\varepsilon}\right) - k_{on} \times \frac{C3}{\varepsilon} \times (Ag - C4) + k_{off} \times C4 \quad (4)$$

$$\frac{dC4}{dt} = k_{on} \times \frac{C3}{\varepsilon} \times (Ag - C4) - k_{off} \times C4 - kint \times C4 \quad , \text{IC} = 0 \quad (5)$$

$$C1 = X1/V1 \quad (6)$$

$$C2 = X2/V2 \quad (7)$$

$$C_{Tumor} = C3 + C4 \quad (8)$$

The model assumes that once the tumor size is small, protein molecules enter tumor interstitial space via surface exchange. When the tumor size is large and vascularized, protein molecules will first distribute to the tumor blood vessels and then extravasate across the tumor microvasculature into the tumor interstitium. (Schmidt and Wittrup, 2009) Equations 2 and 3 describe the plasma PK of protein molecules. Equations 4–8 describe the tumor concentration of protein molecules. P represents the permeability of protein molecules across tumor blood vessels. D is the diffusivity of protein molecules in the tumor interstitium. $\frac{2 \times P \times R_{cap}}{R_k{}^2}$ describes the rate of vascular permeation processes in the tumor blood vessels, where R_{cap} is the radius of tumor blood vessels, and R_k represents the average distance between two tumor blood capillaries. $\frac{6 \times D}{R_t{}^2}$ describes the rate of diffusional transportation of protein molecules by assuming spherical shape of the tumor, where D represents the diffusion coefficient of protein molecules and R_t represents the radius of tumor. $C3$ is the drug concentration in the tissue interstitium. $C4$ is the drug

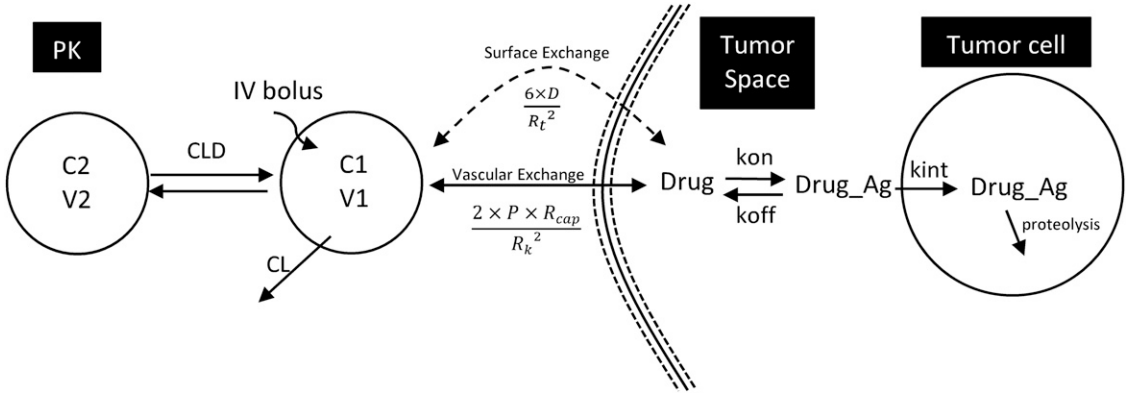

Fig. 1. Schematic of the systems PK model developed to characterize and predict the PK of different-sized protein therapeutics in tumors. The model assumes that after systemic administration, the protein drug can either distribute to the peripheral compartment, clear from the central compartment, or enter tumor interstitial space via surface exchange or vascular exchange. Once in the tumor interstitial space, the protein can bind to the cell- surface antigen. The drug-antigen complex will then internalize into the tumor intracellular space, where the drug is eventually degraded via proteolysis.

TABLE 1

Glossary of the terms used in model equations

Parameter	Description	Unit
X1, X2	Amount of drug in central and peripheral compartments	nmol
C1, C2	Concentration of drug in central and peripheral compartments	nM
C3	Concentration of drug in tumor interstitium	nM
C4	Concentration of cell surface drug-antigen complex	nM
V1, V2	Volume of the central, peripheral compartment	l
C_{tumor}	Tumor concentration of the drug	nM
CLD	Distribution clearance	l/h
CL	Systemic clearance	l/h
TV	Tumor volume	mm^3
R_{cap}	Radius of tumor blood capillary	μm
R_k	Average distance between two capillaries	μm
R_t	Tumor radius	Cm
ε	Void fraction	Unitless
D	Diffusion coefficient	cm^2/h
P	Permeability	μm/h
k_{on}	Association rate between drugs and human epidermal growth factor receptor 2 (HER2)	1/nM per hour
K_D	Dissociation constant between drugs and HER2	pM
k_{off}	Dissociation rate between drugs and HER2	1/h
k_{int}	Internalization rate of the drug-antigen complex	1/h
$Ag_{total,N87}$	Total HER2 concentration on N87 cells	nM
$Ag_{total,468}$	Total HER2 concentration on MDA-MB-468 cells	nM

concentration on the tumor cell surface. Total tumor concentration of the protein drug is represented as the sum of $C3$ and $C4$.

Model Parameters. All model parameters were either measured or derived from literature, and no model parameter was estimated using the observed PK data. These parameters are summarized and presented in Table 2. Diffusion coefficient (D) and permeability (P) were derived based on the reported values of different-sized polymers by Schmidt and Wittrup (2009). The derived relationships between protein size and diffusion coefficient (D) and permeability (P) are listed in eqs. 9 and 10, where the unit of D is square centimeters per hour and unit of P is micrometers per hour A table of calculated value of P and D for different-sized proteins is provided in Supplemental Table 1.

$$D = 114.58 \times MW^{-0.918} \times \frac{3600}{10^7}, \quad \text{MW in kDa} \tag{9}$$

$$P = (-10.43 \times \ln MW + 53.46) \times \frac{3600}{1000}, \quad \text{MW in kDa} \tag{10}$$

Average tumor size in both groups of mice were measured at the time of the experiment and were ~300 mm^3. The equilibrium dissociation constant (K_D) of different-sized proteins for HER2 antigen was measured using the *SPR* method. Dissociation rate constant (k_{off}) was calculated by using the measured K_D value and the reported value of association rate constant (k_{on}). (Shah et al., 2012) The internalization rate of the antigen-protein complex (k_{int}) on N87 cells was taken from reported value by Maass et al. (2016). The number of HER2 receptors per N87 cells were measured in-house. The antigen number of MDA-MB-468 cells was assumed to be 0 since it is known as an HER2-nonexpressing cell line.

Model Simulation and Sensitivity Analysis. Model simulations were performed using Berkeley Madonna (version 8.3.18). No parameter fitting was necessary since all parameter values were a priori determined. Goodness of prediction was assessed by visual check and calculating the percentage prediction error (%PE) for tumor AUC using observed and predicted PK data.

$$PPE = \frac{AUC_{predicted} - AUC_{measured}}{AUC_{measured}} \times 100\% \tag{11}$$

Local sensitivity analysis was done by performing Monte Carlo simulations. The values of parameters P, D, k_{int}, and K_D was varied by 30% CV, and the tumor PK of $F(ab)_2$ was simulated in N87 and MDA-MB-468 tumor-bearing mice.

Results

Synthesis and Characterization of Protein Therapeutics

FcRn nonbinding trastuzumab, $F(ab)_2$, Fab, and scFv fragments of trastuzumab were successfully synthesized. Representative SDS-PAGE

TABLE 2

Model parameter values

Parameter	Value	Unit	Source
R_{cap}	8	μm	From Schmidt and Wittrup (2009), Shah et al. (2012)
R_k	75	μm	From Schmidt and Wittrup (2009), Shah et al. (2012)
R_t	0.42	cm	Measured
ε	0.24	unitless	From Shah et al. (2012)
TV	300	mm^3	Measured
k_{on}	0.259	1/nM per hour	From Shah et al. (2012)
$K_{D\_trastuzumab}$	90	pM	Measured
$K_{D\_F(ab)2}$	42	pM	Measured
K_{D_Fab}	548	pM	Measured
K_{D_scFv}	503	pM	Measured
$k_{off\_trastuzumab}$	0.023	1/h	Calculated
$k_{off\_F(ab)2}$	0.011	1/h	Calculated
k_{off_Fab}	0.14	1/h	Calculated
k_{off_scFv}	0.13	1/h	Calculated
k_{int}	0.035	1/h	From Maass et al. (2016)
$Ag_{total,N87}$	426	nM	Measured
$Ag_{total,468}$	0	nM	Assumed

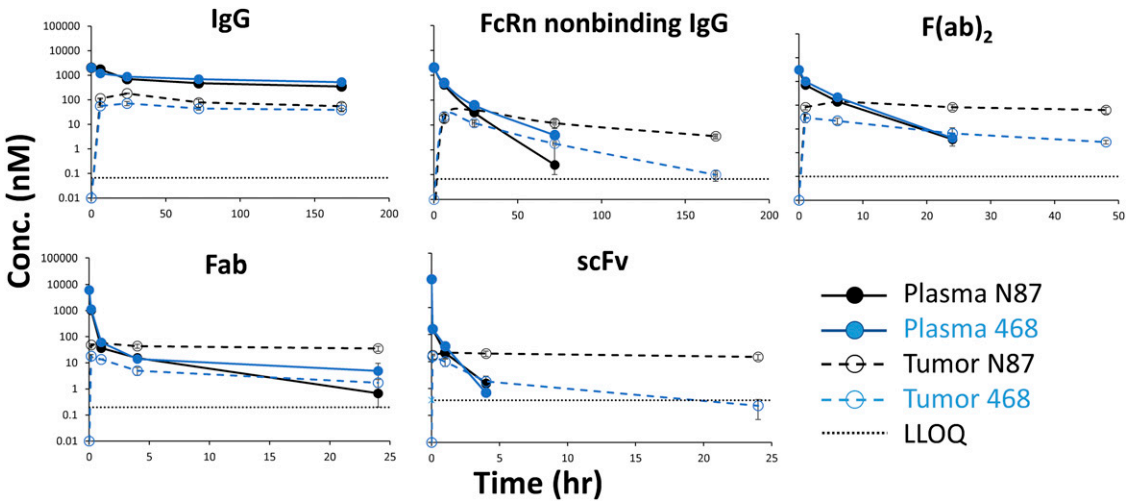

Fig. 2. Plasma and tumor PK profiles of IgG, FcRn-nonbinding IgG, $F(ab)_2$, Fab and scFv in N87, and MDA-MB-468 xenograft-bearing mice. Solid lines represent plasma concentration data. Dashed lines represent tumor concentration data. Black lines represent data from N87 xenografts, and blue lines represent data from MDA-MB-468 xenografts. Black dotted lines represent the lower limit of quantification.

and Western blot analysis figures are provided in Supplemental Fig. 1. HER2-binding affinities of different-sized antibody fragments were determined using SPR. Relative SPR binding curves are shown in Supplemental Fig. 2. K_D values were fitted using Scrubber software (BioLogic Software, Canberra, Australia). Fitted K_D values are summarized in Table 2. The fitting results suggested that scFv and Fab had lower binding affinity, whereas $F(ab)_2$ and trastuzumab had comparable binding affinity. The higher binding affinity of $F(ab)_2$ and trastuzumab may be due to avidity, caused by two binding arms.

Development of ELISA Method to Quantify Different-Sized Protein Molecules in Mouse Plasma and Tumor

Supplemental Figs. 3–6 depicts typical standard curves of trastuzumab, $F(ab)_2$, Fab, and scFv in both mouse plasma and tumor homogenate matrix. All the ELISA protocols enabled quantification of all molecules in both matrices with a lower limit of quantification of 10 ng/ml. Method validation results are provided in Supplemental Table 2.

In Vivo Study to Determine Plasma and Tumor PK of Trastuzumab, FcRn-Nonbinding Trastuzumab, $F(ab)_2$, Fab, and scFv in N87 and MDA-MB-468 Tumor-Bearing Nude Mice. Figure 2 shows the plasma and tumor PK of all five molecules in N87 and MDA-MB-468 tumor-bearing mice. Systemic clearance and terminal half-life values for each molecule were calculated using noncompartmental analysis, which are provided in Table 3. To compare further the effect of protein size on plasma and tumor PK, dose-normalized plasma and tumor PK profiles of all five molecules in two types of tumor-bearing mice are provided in Fig. 3. The plasma PK of each molecule was directly related to molecular size (Figs. 2 and 3). Larger molecules showed slower systemic clearance. For large molecules, such as IgG (150 kDa), systemic clearance was relatively slow, and the terminal half-life was determined to be around 212 hours. For small molecules, such as scFv (27 kDa), drug molecules clear rapidly via renal filtration, and terminal half-life was less than 1 hour. When comparing the plasma PK of same molecule in two different tumor types, tumor antigen expression did not play a significant role in the plasma PK of different size protein molecules. On the other hand, comparison of tumor PK of different-sized antibody fragments (Figs. 2 and 3) showed that all molecules, except IgG, showed significantly different tumor PK between N87 and MDA-MB-468 tumors. In the N87 group, all molecules showed higher tumor concentration, longer tumor retention, and shallower terminal slope, which indicated targeted mediated tumor disposition of the molecules. In HER2 antigen-expressing tumors, the tumor concentration profiles of all molecules followed similar terminal slopes, regardless of protein size (Fig. 3). In contrast, in HER2-nonexpressing MDA-MB-468 tumors, the slope of the tumor concentration profile increased notably with reduction in the size of the molecule.

Figure 4A depicts the observed relationships between maximum tumor uptake and protein molecular weight, which were generated using the PK data obtained from antigen- expressing N87 and antigen-nonexpressing MDA-MB-468 tumors. Wild-type IgG (trastuzumab) was excluded from building this relationship to focus only on the effect of protein size. In both tumor types, maximum tumor uptake showed a positive correlation with protein size in general. Around 100 kDa was the most optimal size to obtain the maximum tumor uptake, especially for antigen-expressing tumors. For small proteins, such as scFv (~27 kDa), tumor maximum uptake did not show a significant difference between two tumor types, possibly owing to rapid plasma clearance; however, for larger proteins with longer plasma half-life, maximum tumor uptake could be significantly different in antigen-expressing (N87) and nonexpressing (MDA-MB-468) tumor types. Higher maximum tumor uptake was observed in tumor types with high antigen expression.

Figure 4B shows the observed relationship between the tumor-to-plasma AUC ratio (0–t) and the protein molecular weight. A "bell" shape relationship was seen in the antigen highly expressing N87 tumor group. In comparison, no such trend was observed in the antigen-nonexpressing MDA-MB-468 tumor group. Around 50 kDa was the optimal size to

TABLE 3

Calculated clearance and half-life of five molecules

Molecule	CL (l/h)	Terminal half-life (h)
Trastuzumab	9.59E−06	212
Neonatal Fc receptor (FcRn)- nonbinding trastuzumab	1.64E−04	6.9
$F(ab)_2$	5.58E−04	3.4
Fab	4.60E−03	4.4
scFv	1.70E−02	0.80

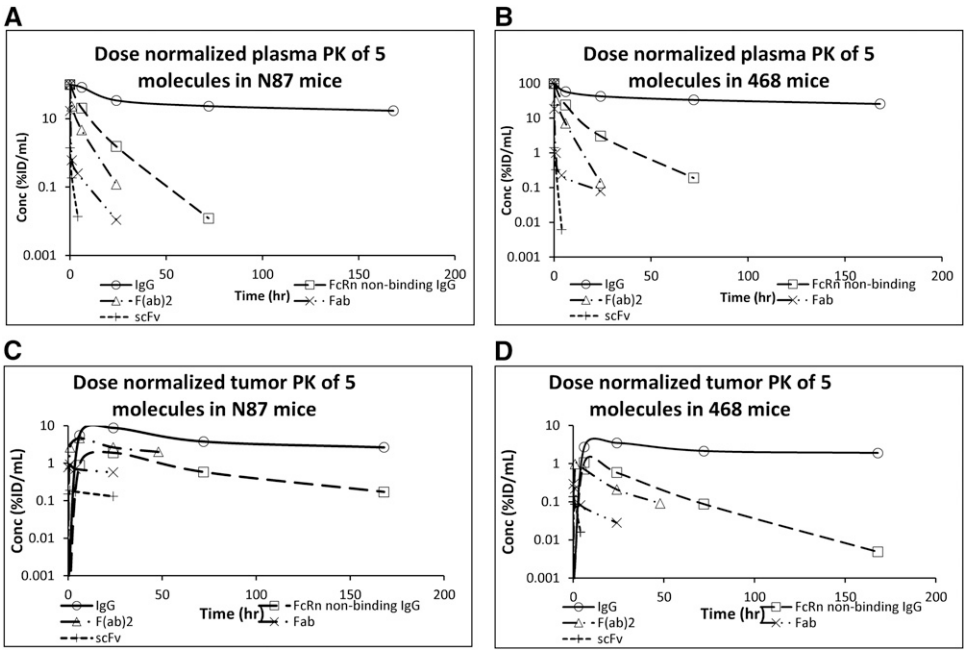

Fig. 3. Dose-normalized plasma PK profiles of IgG, FcRn-nonbinding IgG, $F(ab)_2$, Fab and scFv in (A), N87, and (B) MDA-MB-468 xenograft-bearing mice. Dose-normalized tumor PK profiles of IgG, FcRn-nonbinding IgG, $F(ab)_2$, Fab and scFv in (C) N87, and (D) MDA-MB-468 xenograft-bearing mice. Solid line represents IgG, dashed line represents FcRn-nonbinding IgG, single-dot dashed line represents $F(ab)_2$, double-dot dashed line represents Fab, and dotted line represents scFv.

obtain the maximum tumor-to-plasma AUC ratio, especially for antigen-expressing tumors.

Mathematical Modeling

A Priori Prediction of Tumor PK of Protein Therapeutics in N87 and MDA-MB-468 Tumor-Bearing Mice. Tumor PK of all five molecules in both tumor models was predicted using a two-step sequential approach. First, a two-compartment model was used to fit the plasma PK of each molecule in both types of tumor. Then, the plasma PK model of each molecule was fixed and used to drive the tumor disposition model in both types of tumors. Simulation results are summarized in Figs. 5 and 6. Figure 5 depicts the simulated tumor concentration profile in N87 tumor mice, and Fig. 6 represents MDA-MB-468 mice. The tumor disposition model was able to predict tumor concentration profiles of all molecules in both antigen-expressing N87 and antigen nonexpressing MDA-MB-468 tumors relatively well (within 2- to 3-fold). The %PE values for all the predicted PK profiles are shown in Table 4. Although a slight underprediction was observed for $F(ab)_2$ and Fab PK in N87 tumors, and slight overprediction was observed for IgG and FcRn-nonbinding IgG PK in MDA-MB-468 tumors, this observation may stem from poor accuracy of several reported drug-specific parameters, such as P, D, and k_{int}.

Local Sensitivity Analysis. Local sensitivity analysis of several important parameters (i.e., P, D, k_{int}, and K_D) was conducted using Monte Carlo simulation. Briefly, 30% CV was assumed for each parameter, and the resulting tumor concentration profiles [$F(ab)_2$ as an

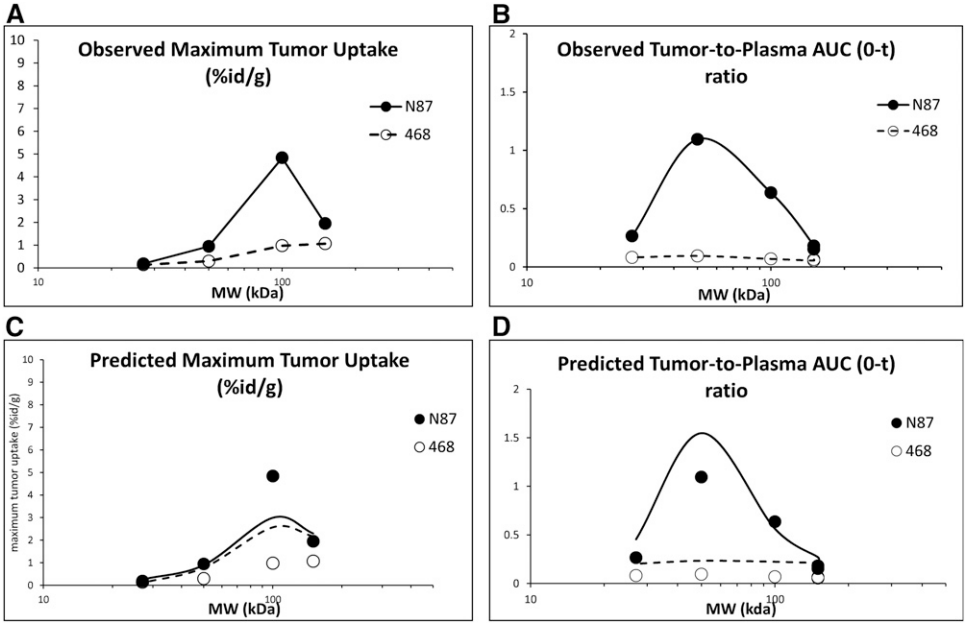

Fig. 4. The relationship between maximum tumor uptake (%id/g) and protein molecular weight (kDa), and tumor-to-plasma AUC (0-t) ratio and protein molecular weight, in N87 and MDA-MB-468 xenograftbearing mice. (A) Observed maximum tumor uptake relationship, (B) observed tumor-to-plasma AUC (0-t) ratio relationship, (C) model predicted maximum tumor uptake relationship, and (D) Model predicted tumor-to-plasma AUC (0–t) ratio relationship. Solid circles and line represent N87 tumor, and open circles and dashed line represent MDA-MB-468 tumor.

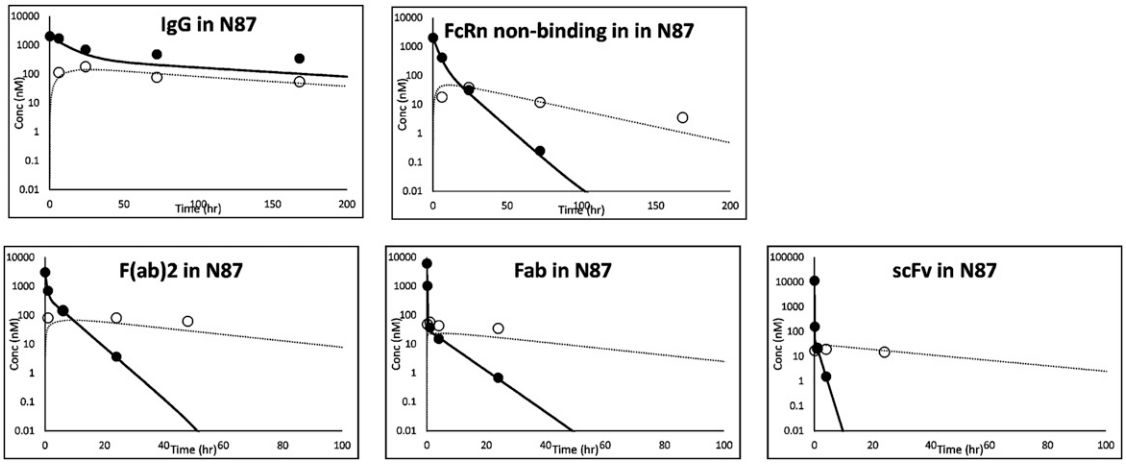

Fig. 5. Tumor PK prediction for IgG, FcRn nonbinding IgG, F(ab)$_2$, Fab and scFv in N87 xenograft-bearing mice. Solid circles represent observed plasma concentration of each molecule. Open circles represent observed tumor concentration of each molecule. Solid line represents model predicted plasma PK profiles of each molecule. Dotted line represents model predicted tumor PK profiles of each molecule.

example] are shown in Fig. 7. In antigen-expressing N87 tumor, the diffusion coefficient (D), permeability (P), and internalization rate (k_{int}) were the most sensitive parameters; however, in antigen nonexpressing MDA-MB-468 tumor, only permeability (P) was sensitive. In N87 tumor, k_{int} greatly influences the terminal slope of the tumor concentration profile, which indicates that k_{int} is the rate-limiting step that determines the tumor exposure in antigen-positive tumor type. From the sensitivity analysis, it was also noticed that K_D was not sensitive for tumor PK in N87 tumors, which may be because all studied molecules bind to HER2 antigen very tightly (in the subnanomolar range), and hence changing K_D value of a molecule by 30% may not significantly affect its tumor PK.

Predicting the Tumor Uptake and Tumor-to-Plasma AUC (0–t) Ratio of Different-Sized Antibody Fragments Using the Tumor PK Model. The tumor model was used to predict maximum tumor uptake and tumor-to-plasma AUC (0–t) ratio of different-sized antibody fragments. Model-simulated relationships are presented in Fig. 4C. The model predicted that the relationship between the maximum tumor uptake versus protein size followed the same trend as the observed data. There was slight deviation between simulated and observed values for several molecules, which was likely due to the difficulty in obtaining accurate maximum tumor uptake data from limited observed time points. Both the observed data and model prediction suggested that F(ab)$_2$ (~100 kDa) would achieve the highest tumor uptake value for fragments without FcRn- binding property. Figure 4D shows the predicted and observed tumor-to-plasma AUC (0–t) ratio versus protein size relationship. For N87 tumor, both the model-predicted and observed relationship showed a bell-shaped relationship between AUC ratio and protein molecular weight. Maximum AUC ratio was predicted to be around 50 kDa. For MDA-MB-468 tumors, model predictions suggested that protein size would not affect AUC ratio, which was consistent with the observed data.

Discussion

Antibody-based molecules have become an essential component of cancer treatment (Tsumoto et al., 2019); however, limited distribution to the site of action has greatly limited the efficacy of antibodies for solid tumors. Several molecular and physicochemical properties govern the

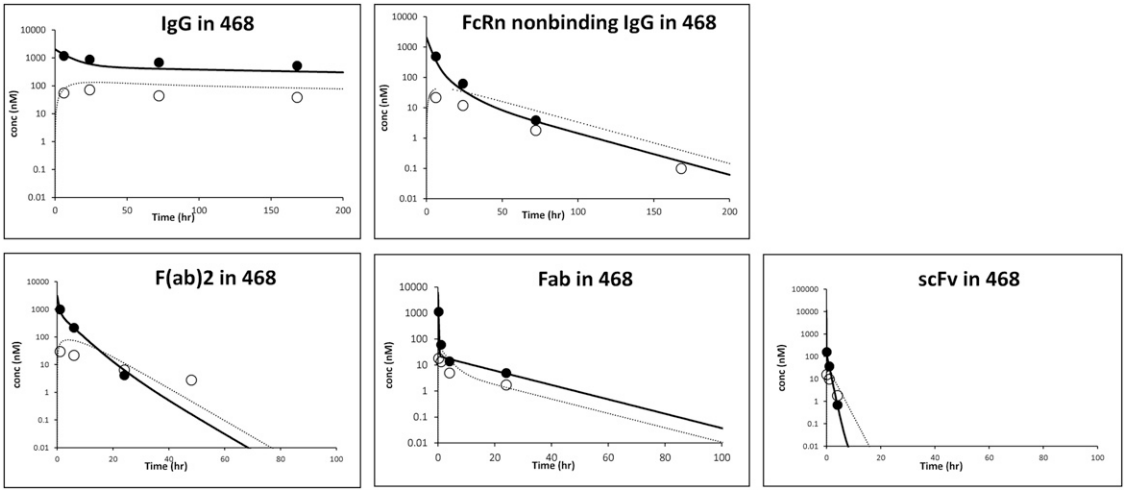

Fig. 6. Tumor PK prediction for IgG, FcRn-nonbinding IgG, F(ab)$_2$, Fab and scFv in MDA-MB-468 xenograft-bearing mice. Solid circles represent observed plasma concentration of each molecule. Open circles represent observed tumor concentration of each molecule. Solid line represents model fitted plasma PK profiles of each molecule. Dotted line represents model predicted tumor PK profiles of each molecule.

TABLE 4

Percentage predictive error (%) for model precited tumor pharmacokinetic profiles

Drug	N87	MDA-MB-468
Trastuzumab	3.96	117
Neonatal Fc receptor (FcRn)-nonbinding trastuzumab	11.9	157
$F(ab)_2$	−22.9	128
Fab	−21.9	87.3
scFv	39.2	21.1

disposition of antibody-based molecules in the tumor, of which molecular size is probably the most important and most extensively studied property. (Beckman et al., 2007). Seeveral different-sized antibody-based constructs have been produced for diagnostic and therapeutic purposes (Beckman et al., 2007); however, to date, no consensus has been reached about the size of protein therapeutics to achieve the desired exposure in the tumor.

Researchers have been studying solid tumor disposition of different-sized protein therapeutics for decades. It is known that diffusion rate of large molecules in tumor is inversely proportional to its molecular size Nugent and Jain (1984). Graff and Wittrup (2003) reported that the diffusion rate of scFv could be six times faster than that of IgG. Therefore, smaller protein molecules, like scFv, presumably would achieve better penetration in the tumor because of faster diffusion; however, tumor exposure of a scFv could also be limited owing to fast systemic clearance and faster diffusion of molecules back into the systemic circulation. The plasma half-life of scFv in mice is typically <2 hours, which limits the time available to this molecule to enter the tumor (Holliger and Hudson, 2005). On the other hand, larger molecules, like full-length antibody, have a prolonged plasma half-life of ~21days in humans and ~7 days in mice. Although this longer circulation half-life provides antibodies more time to enter the tumor, the large size of these molecules hinders their diffusion and limits their exposure in the tumor.

Schmidt and Wittrup (2009) have studied tumor exposure of different-sized (i.e., 10–200 kDa) anti-HER2 molecules in mice and anticarcinoembryonic antigen molecules in humans. They reported a "U"-shape relationship between maximum tumor uptake and molecular weight. In addition, they developed a mathematical model to predict the maximum uptake of different-sized molecules in the tumor. Their model prediction and collected data suggested that a molecular weight of 30–50 kDa would result in least efficient tumor uptake in mice and humans; however, since these inferences were made based on literature reported data collected from diverse sources, and using only the targeted drug molecules, there is a need to verify this important finding further. Consequently, we performed a dedicated tumor disposition study of different-sized variants of the same antibody molecule in target-expressing and target-nonexpressing tumors to obtain more insight into the effect of size on tumor disposition of protein therapeutics.

In the current study, five different molecules were used: trastuzumab, FcRn-nonbinding trastuzumab, $F(ab)_2$, Fab, and scFv. All the variants were produced in the laboratory and buffer exchanged in PBS before use. Whereas the vehicle for trastuzumab is different, and contains commercial formulation, it is safe to assume that the excipients in the commercial formulation would not significantly impact the PK of the antibody. FcRn nonbinding trastuzumab was included in the study to investigate the effect of just the size on tumor PK of antibody and to avoid any confounding effects of FcRn recycling on systemic or tumor disposition of IgGs. Two in vivo tumor models were used: antigen (i.e., HER2) overexpressing N87 cells and antigen-negative MDA-MB-468 cells. Although these two cell lines have different origins (i.e., gastric vs. breast cancer), they satisfied the purpose of this study to decipher the effect of target engagement on tumor PK of different size protein therapeutics. On average, both tumors took 4 to 5 weeks to grow to a volume of ~300 mm^3. As shown in Fig. 2, in the antigen-expressing N87 tumors, all five molecules, except normal IgG, showed significant retention and much shallower terminal slope compared with the plasma; however, in antigen-negative MDA-MB-468 tumors, less retention was observed for all molecules except normal IgG, and the terminal slopes of all molecules changed commensurately with changes in the plasma PK profiles. This observation suggests that when there is no target-binding process in the tumor, the rate-limiting step that governs tumor concentration is the plasma PK of the drug. On the other hand, when the drug molecules bind to tumor cell-surface antigens, the rate-limiting step is determined by the slowest of the following processes: drug dissociation rate from the antigen (k_{off}), internalization rate of the drug (k_{int}), and systemic clearance. In the case of normal IgG, plasma PK becomes the rate-limiting step in both N87 and MDA-MB-468 tumor models, and hence parallel plasma and tumor concentration profiles are observed.

When dose-normalized plasma PK profiles of all five molecules in N87 and MDA-MB-468 tumor models were compared (Fig. 3, A and B), plasma half-life decreased with decreasing protein molecular size in both tumor models. Normal IgG (~150 kDa) had longest plasma half-life (~10 days) in both tumor models. The calculated clearance (CL) of normal IgG was around 1.0E−05 l/h, which is close to the average

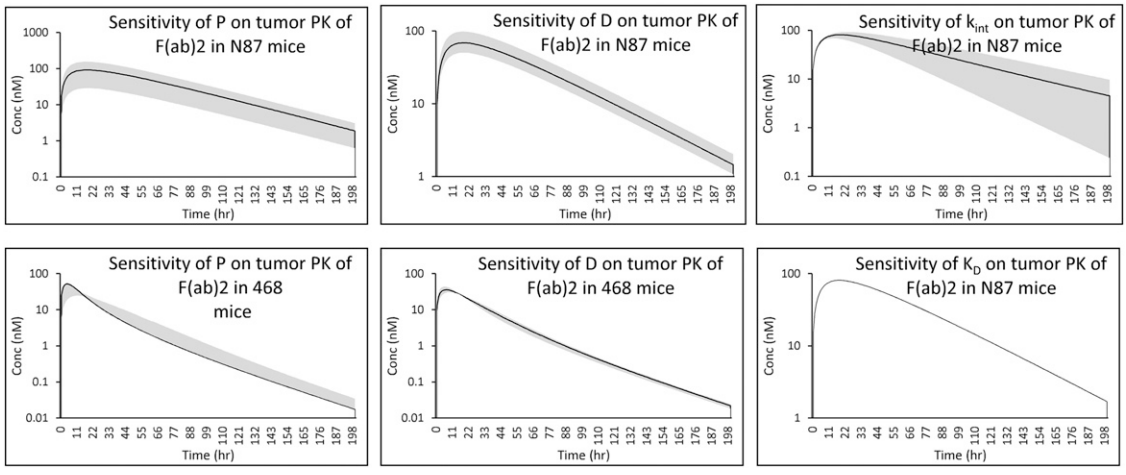

Fig. 7. Local sensitivity analysis, where P, D, kint, and KD are changed by 30% CV to evaluate the effect on the PK of $F(ab)_2$ fragment in N87 and MDA-MB-468 tumors.

calculated values from the literature-reported PK data of IgGs in mice (1.6E−05 l/h). (Li et al., 2017). For FcRn nonbinding IgG (~150 kDa), the plasma half-life was similar in both tumor models (~8 hours). The calculated CL value was 1.5E−04 l/h, which was about 3-fold greater than the reported value of murine IgG in FcRn knockout mice (5.2E−05 l/h). (Garg and Balthasar, 2007). For smaller proteins, such as $F(ab)_2$ (~100 kDa) and Fab (~50 kDa), the observed half-life was around 3–5 hours in both tumor models. The calculated CL values for $F(ab)_2$ and Fab were 4.2E−04 and 4.6E−03 l/h, respectively. These values are also close to the calculated values from the collected PK studies of $F(ab)_2$ and Fab in mice (4.4E−04 and 2.7E−03 l/h, respectively) in the literature (Li et al., 2017). The smallest molecule, scFv (~27 kDa), had a plasma half-life of less than 1 hour (~0.5 hour) in both tumor models. The calculated CL value for scFv was 1.5E−02 l/h, which was roughly 10-fold higher than the calculated value from the literature collected studies (1.6E−03 l/h). (Li et al., 2017) Of note, to avoid any confounding effect of labeling and label-based analytical methods, here we have quantified all the molecules using a validated ELISA method. As such, the reported PK parameters may differ from the one generated using labeled molecules.

Figure 3, C and D, shows dose-normalized tumor concentration profiles of all five molecules in N87 and MDA-MB-468 tumor-bearing mice. In both tumor groups, there was a general trend of increasing tumor maximum uptake with increasing protein molecular size. The only exception is $F(ab)_2$ in the N87 group, which has a higher tumor maximum uptake compared with FcRn-nonbinding IgG. In the N87 group, the terminal slopes of tumor concentration profiles of all five molecules are relatively similar. Given the fact that the binding affinities of these five molecules against recombinant HER2 protein are different (as determined using the SPR method), the parallel terminal slopes suggest that the rate-limiting step for the tumor PK of all molecules is likely the internalization rate (k_{int}) of the drug-antigen complex. On the other hand, in the MDA-MB-468 group, the terminal slopes increased with decreasing protein molecular size, which suggests that the rate-limiting step in antigen-negative tumor is the plasma clearance of the molecules. In Fig. 4A, the observed relationships between maximum tumor uptake and protein molecular weight are shown. Compared with the "U"-shape relationship reported by Schmidt and Wittrup (2009), the result from the current study agrees relatively well with the right half of the relationship, which suggests that further study with smaller antibody fragments (e.g., nanobody, ~13 kDa) is needed. It should be noted that in Fig. 4A, only FcRn-nonbinding molecules demonstrate just the effect of molecular size on tumor disposition of protein therapeutics. When wild-type trastuzumab is included in the analysis, because of its longer half-life resulting from FcRn interaction, it has the highest peak concentrations in the tumor (i.e., 9 %id/g). In Fig. 4B, the relationships between tumor-to-plasma AUC (0-t) ratio and protein molecular weight are shown. The result suggests that the highest tumor-specific exposure occurs at a molecular weight of ~50 kDa for antigen-positive tumors. Larger molecules suffer from a delivery barrier at the local tumor site, whereas smaller molecules suffer from rapid systemic clearance. This result could be potentially helpful in designing an optimal size tumor diagnostic agent, which requires high tumor-to-background ratio. On the other hand, in the antigen-negative MDA-MB-468 tumor group, the result suggest that the tumor-to-plasma AUC ratio is independent of protein molecular size, which is expected because no tumor retention was observed in this group.

To understand more completely the relationship between tumor disposition and protein molecular size in both antigen-positive and -negative tumors, a tumor PK model was developed. As shown in Figs. 5 and 6, the model was able to predict a priori the tumor concentration of all five molecules in both types of tumors relatively well. Since no drug-related parameter or system related parameter is fitted in the tumor model, these predictions suggest that the current tumor model is a robust tool to predict tumor concentration profiles of different-sized antibody fragments. To understand better the effect of several important drug-related and tumor-related parameters (e.g., P, D, k_{int}, and K_D) on the tumor PK of different-sized protein molecules, local sensitivity analysis was conducted (Fig. 7). The result suggests that for therapeutic antibodies/fragments that have strong binding with the tumor cell-surface antigen (K_D in subnanomolar range), a further increase in binding would have little improvement in overall tumor exposure. On the other hand, the properties of the internalization rate (k_{int}) of the cell-surface antigen might play a pivotal role in determining the tumor concentration of a drug. The sensitivity analysis also reveals that the molecular size influences tumor disposition of proteins by affecting both its plasma PK and disposition properties (e.g., P, D) in the tumor microenvironment. The results of the tumor PK model simulation suggest that the cell-surface antigen expression level is a sensitive parameter only in antigen low-expressing tumors. In the current study, since the antigen expression level is high in N87 cells (426 nM) and fast turnover is assumed, the applied dose (10 mg/kg) will not saturate all binding sites on the cell surface, and therefore the tumor PK profile is insensitive to antigen level. The linearity of the tumor PK depends on several antigen-binding related parameters, such as K_D, k_{int}, tumor size, and cell-surface antigen expression level. In the current study, nonlinear PK is not predicted until the dose exceeds 5 mg/kg. Using this tumor PK model, the maximum tumor uptake versus the protein molecular weight relationship and the tumor-to-plasma AUC ratio versus protein molecular weight relationship were also predicted and compared with the observed data. Whereas the model-predicted relationships agreed well with the observed trends from the data, more data from different-sized molecules are required to validate the model and observed trends. Nonetheless, the systems PK model presented here provides a platform to predict the PK of different-sized protein therapeutics in preclinical and clinical tumors.

In summary, here we have presented a preclinical in vivo investigation to study the effect of size on tumor disposition of protein therapeutics. Our results suggest that the tumor PK of different-sized protein therapeutics can differ greatly between antigen- expressing and nonexpressing tumors. We observed parallel terminal slopes for all sizes of molecules in antigen-expressing tumors, and tumor slopes of these molecules matched their plasma terminal slopes in antigen nonexpressing tumors. We also observed that ~100 kDa is an optimal size to achieve peak tumor concentration for non-FcRn binding targeted drug molecules, and ~50 kDa is an optimal size to achieve the maximum tumor-to-plasma exposure ratio. All the observed PK data were a priori predicted by a systems PK model developed to characterize tumor disposition of different-sized protein therapeutics. Such tumor PK models provide a quantitative framework for discovery, development, and preclinical-to-clinical translation of different-sized therapeutic and diagnostic agents.

Authorship Contributions

Participated in research design: Z. Li, Shah.
Conducted experiments: Z. Li, Y. Li, Chang.
Contributed new reagents or analytic tools: Z. Li, Y. Li, Chang, Guo.
Performed data analysis: Z. Li, Shah.
Wrote or contributed to the writing of the manuscript: Z. Li, Shah.

References

Beckman RA, Weiner LM, and Davis HM (2007) Antibody constructs in cancer therapy: protein engineering strategies to improve exposure in solid tumors. *Cancer* **109**:170–179.

Garg A and Balthasar JP (2007) Physiologically-based pharmacokinetic (PBPK) model to predict IgG tissue kinetics in wild-type and FcRn-knockout mice. *J Pharmacokinet Pharmacodyn* **34**:687–709.

Glassman PM and Balthasar JP (2014) Mechanistic considerations for the use of monoclonal antibodies for cancer therapy. *Cancer Biol Med* **11**:20–33.

Graff CP and Wittrup KD (2003) Theoretical analysis of antibody targeting of tumor spheroids: importance of dosage for penetration, and affinity for retention. *Cancer Res* **63**:1288–1296.

Holliger P and Hudson PJ (2005) Engineered antibody fragments and the rise of single domains. *Nat Biotechnol* **23**:1126–1136.

Li Z, Krippendorff B-F, and Shah DK (2017) Influence of molecular size on the clearance of antibody fragments. *Pharm Res* **34**:2131–2141.

Li Z, Krippendorff B-F, Sharma S, Walz AC, Lavé T, and Shah DK (2016) Influence of molecular size on tissue distribution of antibody fragments, *MAbs* **8**, pp 113–119.

Maass KF, Kulkarni C, Betts AM, and Wittrup KD (2016) Determination of cellular processing rates for a trastuzumab-maytansinoid antibody-drug conjugate (ADC) highlights key parameters for ADC design. *AAPS J* **18**:635–646.

Nugent LJ and Jain RK (1984) Extravascular diffusion in normal and neoplastic tissues. *Cancer Res* **44**:238–244.

Schmidt MM and Wittrup KD (2009) A modeling analysis of the effects of molecular size and binding affinity on tumor targeting. *Mol Cancer Ther* **8**:2861–2871.

Scott AM, Wolchok JD, and Old LJ (2012) Antibody therapy of cancer. *Nat Rev Cancer* **12**: 278–287.

Shah DK, Haddish-Berhane N, and Betts A (2012) Bench to bedside translation of antibody drug conjugates using a multiscale mechanistic PK/PD model: a case study with brentuximab-vedotin. *J Pharmacokinet Pharmacodyn* **39**:643–659.

Thurber GM, Schmidt MM, and Wittrup KD (2008a) Antibody tumor penetration: transport opposed by systemic and antigen-mediated clearance. *Adv Drug Deliv Rev* **60**:1421–1434.

Thurber GM, Schmidt MM, and Wittrup KD (2008b) Factors determining antibody distribution in tumors. *Trends Pharmacol Sci* **29**:57–61.

Thurber GM, Zajic SC, and Wittrup KD (2007) Theoretic criteria for antibody penetration into solid tumors and micrometastases. *J Nucl Med* **48**:995–999.

Tsumoto K, Isozaki Y, Yagami H, and Tomita M (2019) Future perspectives of therapeutic monoclonal antibodies. *Immunotherapy* **11**:119–127.

Wang W, Wang EQ, and Balthasar JP (2008) Monoclonal antibody pharmacokinetics and pharmacodynamics. *Clin Pharmacol Ther* **84**:548–558.

Address correspondence to: Dr. Dhaval K. Shah, Department of Pharmaceutical Sciences, 455 Kapoor Hall, School of Pharmacy and Pharmaceutical Sciences, University at Buffalo, The State University of New York, Buffalo, New York 14214-8033. E-mail: dshah4@buffalo.edu